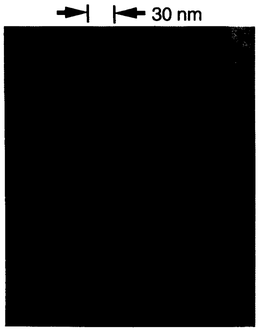

Fig. 7. SEM micrograph of metal lines fabricated by imprint lithography and a lift-off process. The lines are 30 nm wide and have a period of 70 nm.

ations on the mold sidewall could be faithfully imprinted into the PMMA; this observation showed that the minimum linewidth that can be achieved with imprint lithography is limited by mold size. With a suitable mold, 10-nm-wide PMMA lines or trenches may be fabricated by means of imprint lithography.

To examine the extent to which the oxygen RIE pattern transfer step removed the residual resist in the compressed areas and changed the lateral dimension of the PMMA features, we used the PMMA resist structures created by imprint lithography as the template for a lift-off of metals. In the lift-off process, 5 nm of Ti and 15 nm of Au were first deposited onto the entire sample, and then the metal on the PMMA surface was removed when the PMMA was dissolved in acetone. We compared the SEM image of the imprinted PMMA template before the oxygen RIE transfer to that of the metal patterns after the lift-off. SEM micrographs of the metal dots (Fig. 5) and lines (Fig. 6) that were fabricated with the PMMA templates shown in Figs. 2 and 3, respectively, show that the lift-off metal has the same feature size as the original molded PMMA structures. Hence, during the oxygen RIE process, the compressed PMMA area was completely removed and the lateral size of the PMMA features did not change noticeably. Finally, we used imprint lithography and lift-off to fabricate 30-nm-wide metal lines with a 70-nm period (Fig. 7). This SEM micrograph indicates that although the PMMA template cannot be directly seen with SEM because of electron beam–induced melting, 30-nm-wide trenches with a 70-nm period were indeed made in PMMA by means of imprint lithography.

Imprint lithography offers many advantages over conventional lithographies. First, imprint lithography abandons the use of an energetic beam of electrons, photons, or ions, which creates a chemical structure contrast in a resist. Instead, imprint lithography uses compression molding to create a thickness contrast in a resist. As a result, imprint lithography eliminates many factors that limit the resolution of conventional lithographies, such as wave diffraction, scattering in the resist, backscattering from substrate, and chemistry of resists and developers. Second, imprint lithography not only can have 25-nm resolution, but also can print a large area at once, therefore offering a high throughput. Third, its cost is potentially low because it does not require a sophisticated energetic beam generator. We believe that with further development, such as optimization of the polymer resist and mold materials and of the compression conditions, large areas (greater than 50 mm by 50 mm) of sub–25-nm imprint lithography should be achievable without the sticking and defect problems associated with traditional contact printing. These developments would make imprint lithography a viable technology for manufacturing 25-nm structures.

REFERENCES AND NOTES

1. A. N. Broers, J. M. Harper, W. W. Molzen, *Appl. Phys. Lett.* **33**, 392 (1978); P. B. Fischer and S. Y. Chou, *ibid.* **62**, 2989 (1993).
2. D. Flanders, *ibid.* **36**, 93 (1980); K. Early, M. L. Schattenburg, H. I. Smith, *Microelectron. Eng.* **11**, 317 (1990).
3. M. A. McCord and R. F. P. Pease, *J. Vac. Sci. Technol.* **B4**, 86 (1986); J. W. Lyding, T. C. Shen, J. S. Hubacek, J. R. Tucker, G. C. Abelin, *Appl. Phys. Lett.* **64**, 2010 (1994); N. Kramer, M. Birk, J. Jorvitsma, C. Schronenberger, *ibid.* **66**, 1325 (1995).
4. M. Harmening *et al.*, *Proceedings IEEE Micro Electro Mechanical Systems* (IEEE, Piscataway, NJ, 1992), p. 202.
5. H. Li and S. D. Senturia, *Proceedings of the 13th IEEE/CHMT International Electronic Manufacturing Technology Symposium* (IEEE, Piscataway, NJ, 1992), p. 145.
6. I. Rubin, *Injection Molding* (Wiley, New York, 1972).
7. We thank other members of the NanoStructure Laboratory whose efforts have profoundly affected the current work. S.Y.C. thanks W. T. Peria for suggesting the term thickness-contrast lithography as an alternative name for imprint lithography. Supported in part by the Packard Foundation through a Packard fellowship.

12 December 1995; accepted 12 February 1996

Autocatalysis During Fullerene Growth

B. R. Eggen,* M. I. Heggie, G. Jungnickel, C. D. Latham,
R. Jones, P. R. Briddon

Total energy calculations with a local spin density functional have been applied to the Stone-Wales transformation in fullerene (C_{60}). In the formation of the almost exclusively observed I_h isomer of C_{60} with isolated pentagons, the final transformation must be from a C_{2v} isomer with two pentagon pairs. It was found that the energy barrier for this rearrangement was substantially reduced in the presence of an extra carbon atom. Such atoms were found to bind loosely, preferentially to regions in which there were paired pentagons. Pentagon rearrangements, which are necessary steps in the growth of fullerenes, may therefore result from autocatalysis by carbon.

One of the great surprises in fullerene chemistry has been that only one isomer of C_{60} is isolated in macroscopic quantities—that having I_h symmetry and hence satisfying the isolated pentagon rule (*1*). Evidence for defect isomers is scarce, although they have been observed with scanning-tunneling microscopy (*2*). Whereas this can be understood in broad terms on energetic grounds (*1*)—the observed structure is undeniably the lowest energy isomer—other isomers have energies within 1.5 eV of it, and it is not evident that this energy difference alone would rule out their occurrence in observable quantities. The energy difference is only 0.03 eV per atom, a value similar to the difference in cohesive energy between diamond and graphite (*3*), which does not preclude the existence of diamond as a kinetically stable phase. Furthermore, C_{60} isomers are most likely to interconvert through the Stone-Wales (SW) (*4*) (also known as pyracylene) transformations (Fig. 1), which have been shown by reliable theoretical methods to give rise to extremely high-energy barriers of 6 to 7 eV (*5–8*). The C_{2v} C_{60} isomer with two adjacent pentagon pairs is a bottleneck in the SW transformations scheme that connects most of the possible C_{60} isomers, because any SW route to the I_h C_{60} fullerene has to encounter it in the ultimate step (*9*); this last step is the subject of this report.

We have shown that interaction between C_{60} and H can cause the I_h C skeleton to be higher in energy than a D_{6h}

B. R. Eggen and M. I. Heggie, School of Chemistry and Molecular Sciences, University of Sussex at Brighton, Falmer, BN1 9QJ, UK.
G. Jungnickel, Institut für Physik, Theoretische Physik III, Technische Universität Chemnitz-Zwickau, D-09107 Chemnitz, Germany.
C. D. Latham and R. Jones, Department of Physics, University of Exeter, Exeter, EX4 4QL, UK.
P. R. Briddon, Department of Physics, University of Newcastle, Newcastle, NE1 7RU, UK.

*To whom correspondence should be addressed.

skeleton (for the molecule $C_{60}H_{12}$) (*10*). We investigated the possibility that H could catalyze the SW transformations, in order to gauge whether the D_{6h} isomer of $C_{60}H_{12}$ might be observable. In the presence of an H atom, the SW barrier in C_{60} was reduced from 6.2 to 4.6 eV (*7*). The H atom destabilized the reactants and products and stabilized the transition state. We also found indications that the barrier may be reduced further to 4.1 eV, given the less probable circumstance of two H atoms being involved, but we did not perform an exhaustive search for the saddle point state.

However, although it is always possible that trace amounts of H are present during fullerene formation—normally as water, which is extremely difficult to expunge totally from glassware—it is known that the presence of significant amounts of H can extinguish the growth process (*11*). A more likely situation is that individual C atoms are produced under the extreme conditions that prevail at the electrodes, and that these are associated transiently with the C_{60} (or indeed any fullerene) shell. Here we present total energy calculations for structures and energy paths involving C_{60} and C. In embarking on these calculations, we were guided by experimental evidence that shows that a low-energy ^{13}C ion impinging on a $^{12}C_{60}$ molecule can be absorbed into the C skeleton with the consequent emission of a ^{12}C ion (*12*).

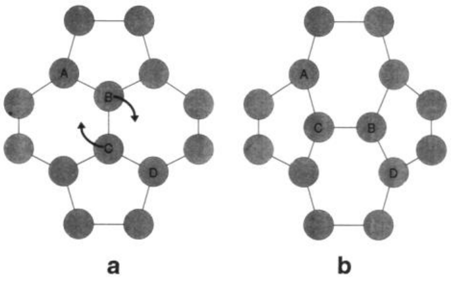

Fig. 1. In the SW transformation (**a** to **b**), two C atoms (labeled B and C) rotate by 90° about the center of their mutual bond, rearranging hexagons and pentagons.

In our computer modeling we used a parameter-free method of solving the many-body Schrödinger equation that is extremely efficient for clusters of up to 1000 *p*-block element atoms (*13*–*15*). The model invokes the local spin density approximation for exchange and correlation within the density functional technique [using the Ceperley-Alder functional (*16*)]. Only valence electrons were considered, atom cores being replaced with norm-conserving pseudopotentials (*17*). A real-space basis of 16 Gaussians per atom (four each as *s*, p_x, p_y, p_z variants) for the molecular wave functions and *s*-only Gaussians to fit the valence charge density (four per C atom) was used. Forces on the atoms were calculated analytically, and we optimized structures using a conjugate gradient method until these forces were negligible.

The method has been shown to reproduce many features of fullerenes, most notably the vibrational modes of C_{60} (*18*, *19*) and the interaction of C_{60} with H (*10*, *20*). By way of illustration, the D_{5h} isomer of C_{70} is found to be lower in energy by 0.029 eV per atom than I_h C_{60}, compared with the calorimetric value of 0.023 eV per atom (*21*).

For the study of saddle points, a constraint technique was used, which removes two degrees of freedom from the system (the "reaction coordinates"), plots an energy surface for those two degrees (allowing structural optimization of all other degrees of freedom), and locates the saddle point graphically from that surface. In all calculations presented here, a surface generated from at least 50 points in the two-dimensional space was used, with enhanced density around the saddle point. In the SW transformation there are four "active" atoms, labeled A to D in Fig. 1. The process requires that bonds A–B and C–D are broken (Fig. 1a) and bonds A–C and B–D are formed (Fig. 1b), and we define the two reaction coordinates as $r^2_{AB} - r^2_{BD}$ and $r^2_{AC} - r^2_{CD}$. Figure 2 shows the resultant energy surface, from which an activation energy of 6.2 eV can be deduced, corresponding to constraints of (0,0). In the saddle point structure, the bond B–C tends toward triple character and there are dangling sp^2 hybrids on A and D that can be stabilized by H. Our calculation shows no evidence of an "asymmetric" saddle point (*6*), even though such structures are allowed by our constraint and we did examine asymmetric starting points.

We examined the ground states of C_{61} from five different starting points. The two lowest lying energy minima were identified as radially displaced bond-center sites, above the hexagon-hexagon (h-h) fusion and hexagon-pentagon (h-p) fusion bonds. Their formation energies with respect to a C atom at infinity and the optimized I_h C_{60} framework were −3.09 eV for the h-h site (structure GS of Fig. 3) and −2.83 eV for the h-p site. The former

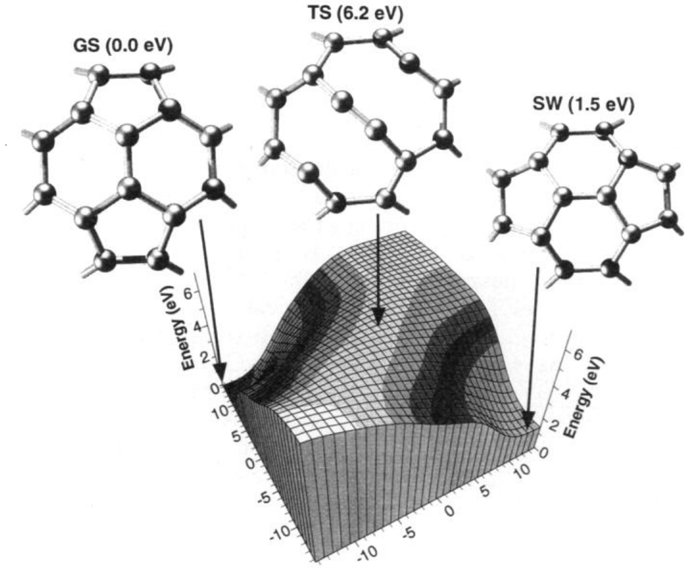

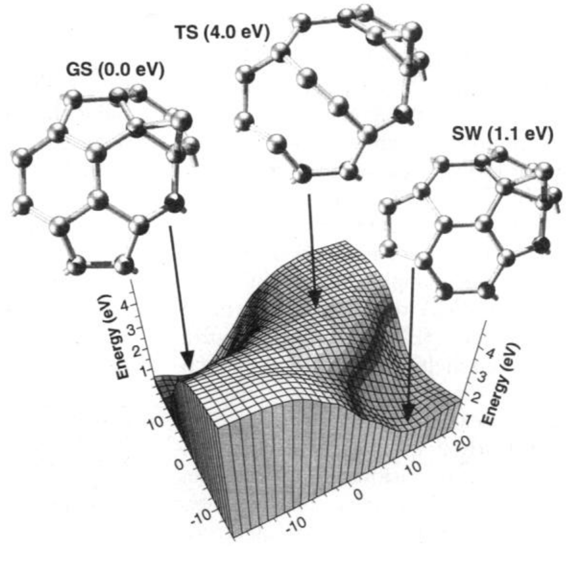

Fig. 2 (left). Local density functional (LDF) energy surface for the constrained SW reaction path for C_{60}; energy is plotted against values of the two constraints. **Fig. 3 (right).** The LDF energy surface for the constrained SW reaction path for C_{61}; energy is plotted against values of the two constraints. The insets show the associated SW, GS, and TS structures.

structure (the methano-isomer) has C_{2v} symmetry with the extra C atom involved in an almost perfect equilateral triangle of bonding (bond lengths, 1.50 Å; angle, 61°). The latter (the homo-isomer) has C_s symmetry with the extra C having bonds of 1.43 Å and an included angle of 100°. We confirmed the mobility of the extra C atom by applying a double constraint on the methano- to homo-isomer conversion of C_{61} and finding an activation energy of only 1.1 eV (implying that motion of the extra C atom around the C_{60} cage will be relatively easy and not rate-limiting for any of the following processes).

Our calculations, which are spin-polarized, disagree with results obtained with the AM1 semiempirical quantum-chemical package (*22*), which suggested that the singlet C_s C_{61} isomer is more stable than the C_{2v} C_{61} isomer. In addition we examined the triplet states of each of our ground-state structures and always found them to be higher in energy than the singlet states. The lowest singlet:triplet energy difference was 0.12 eV for the C_s C_{61} structure.

In investigating the possible products of the SW transformation (starting from the C_{2v} C_{60} fullerene with neighboring pentagons) in the presence of the extra C atom, we considered only those off–bond center sites that neighbor the four "active" atoms. By symmetry, this means the three bonds neighboring atom D (ignoring the bond center between atoms B and C, which we believe will have little effect on the SW transformation energy). Placing the extra C atom on the bonds to atom D, we found three isomers within 0.5 eV of each other. The lowest energy structure (structure SW of Fig. 3) was 1.09 eV less stable than methano-C_{61} and the off–bond center site was located on the h-h bond of the original I_h C_{60} cage. The product of an SW transformation on I_h C_{60} is a C_{2v} isomer with an energy 1.47 eV greater than that of I_h; clearly, the product isomer binds the extra C atom more strongly, by some 0.4 eV, than the I_h isomer.

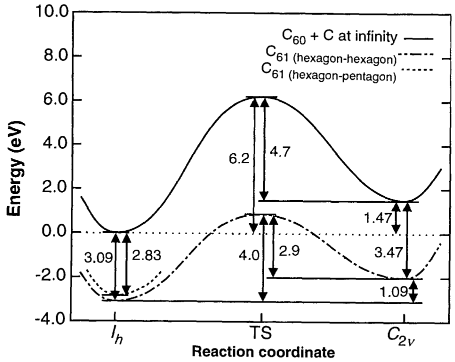

Fig. 4. Schematic LDF energy diagram for the SW reaction path for C_{60} and C_{61}; energy is plotted against an arbitrary reaction coordinate.

We investigated the route between the methano-isomer and the lowest energy product in the same fashion as for C_{60}. Initial placement of the extra C atom (before each constrained structural optimization) was radially outward from atom D. Care was taken to ensure that the final position of the extra C atom, whose position was unconstrained, did not vary by large amounts between different points on the energy surface; such movements would have indicated a poor choice of constraints and a double-valued energy surface. At every point on the energy surface we investigated, the extra C atom took up an off–bond center position in the same bond neighboring atom D.

The resulting energy surface (Fig. 3) exhibited a saddle point (or transition state) of 4 eV (structure TS of Fig. 3), well below that for C_{60}. Because of the presence of the extra C atom bonded to atom D, the saddle point was asymmetric and fairly broad and flat. The structures with positive constraint values tended to be lower in energy than corresponding negative values, because the rotating C_2 unit (B–C) with a triple bond and the extra C atom with a double bond repel each other (structure TS of Fig. 3). It is not possible to interpret the energy lowering as easily as in the H case, but it seems that the extra C atom can bond more strongly to the saddle point structure than to C_{60}, principally through increased bond order on one side. Farther away from structure TS we found structures that may lead to exchange of the extra C atom with a host C; perhaps these structures are responsible for the isotope scrambling experiments (*12*).

With reference to an isolated I_h C_{60} molecule and C atom, the ground state of C_{61} is the methano-isomer, at −3.07 eV. The activation energy of the associated SW reaction is significantly lowered from more than 6 eV for the uncatalyzed transformation to 4 eV for the autocatalyzed one (Fig. 4). Crucial to the fullerene pathway for C_{60} formation is the reverse of this reaction, which removes the paired pentagons from the C_{2v} C_{60} isomer, with a barrier of only 2.9 eV. Because SW transformations are necessary for the "fullerene pathway" growth mechanism, their catalysis by C therefore constitutes autocatalysis of the C cluster growth process.

The extra C atom has the mobility (activation energy of 1.1 eV) and thermodynamic bias (extra binding of 0.4 eV) to seek out paired pentagon regions and adopt a configuration favorable to the catalysis of the SW transformation. If this reaction is typical of other SW transformations, this could be a general mechanism for fullerene annealing and could be the cause of the 1200°C lower bound on the annealing temperature for efficient formation of C_{60} in the gas phase (*23*).

Although there is clearly a strong thermodynamic bias for either the removal of the extra C atom into a more strongly bound structure or for the incorporation of a further C atom, it is not unrealistic to expect that in the gas phase the C_{61} molecule could remain out of thermodynamic equilibrium with the reservoir of C for extended periods, enabling catalysis to occur. During collisions, the extra C atom should transfer from the annealed I_h isomer to an unannealed paired pentagon isomer, sustaining the catalytic action.

REFERENCES AND NOTES

1. H. W. Kroto, J. R. Heath, S. C. O'Brien, R. F. Curl, R. E. Smalley, *Nature* **318**, 162 (1985).
2. P. K. Dutta, S. B. Samanta, A. V. Narlikar, *Philos. Mag. Lett.* **67**, 101 (1993).
3. M. T. Yin and M. L. Cohen, *Phys. Rev. B* **29**, 6996 (1984).
4. A. J. Stone and D. J. Wales, *Chem. Phys. Lett.* **128**, 501 (1986).
5. J.-Y. Yi and J. Bernholc, *J. Chem. Phys.* **96**, 8634 (1992).
6. R. L. Murry, D. L. Strout, G. K. Odom, G. E. Scuseria, *Nature* **366**, 665 (1993).
7. M. I. Heggie, C. D. Latham, R. Jones, P. R. Briddon, in *Fullerenes: Chemistry, Physics, and New Directions VII*, K. M. Kadish and R. S. Ruoff, Eds. (Electrochemical Society, Pennington, NJ, 1995), pp. 1218–1223.
8. B. R. Eggen, M. I. Heggie, C. D. Latham, R. Jones, P. R. Briddon, *Synth. Metals*, in press.
9. S. J. Austin, P. W. Fowler, D. E. Manolopoulos, F. Zerbetto, *Chem. Phys. Lett.* **235**, 146 (1995).
10. M. I. Heggie, R. Jones, P. R. Briddon, in *Recent Advances in the Chemistry and Physics of Fullerenes and Related Materials*, K. M. Kadish and R. S. Ruoff, Eds. (Electrochemical Society, Pennington, NJ, 1994), pp. 307–316.
11. X. K. Wang *et al.*, *J. Mater. Res.* **10**, 1977 (1995).
12. J. F. Christian, Z. M. Wan, S. L. Anderson, *J. Phys. Chem.* **96**, 3574 (1992).
13. R. Jones and A. Sayyash, *J. Phys. C* **19**, 653 (1986).
14. R. Jones, *ibid.* **21**, 5735 (1988).
15. ———, *Mol. Simulation* **4**, 113 (1989).
16. D. M. Ceperley and B. J. Alder, *Phys. Rev. Lett.* **45**, 566 (1980).
17. G. B. Bachelet, D. R. Hamann, M. Schlüter, *Phys. Rev. B* **26**, 4199 (1982).
18. J. C. R. Faulhaber, D. Y. K. Ko, P. R. Briddon, *ibid.* **48**, 661 (1993).
19. R. Jones *et al.*, *Philos. Mag. Lett.* **65**, 291 (1992).
20. S. K. Estreicher, C. D. Latham, M. I. Heggie, R. Jones, S. Öberg, *Chem. Phys. Lett.* **196**, 311 (1992).
21. H.-D. Beckhaus *et al.*, *Angew. Chem. Int. Ed. Engl.* **33**, 996 (1994).
22. Z. Slanina and S. L. Lee, *Thermochem. J. Mol. Struct.* **110**, 173 (1994).
23. R. E. Smalley, *Acc. Chem. Res.* **25**, 98 (1992).
24. This research was supported by the United Kingdom Science and Engineering Research Council (especially its Computational Science and its High Performance Computing Initiatives). B.R.E. received additional support from the Royal Society of Great Britain (grant 574005.G501). We thank H. W. Kroto, J. P. Hare, and P. W. Fowler for helpful discussions.

18 December 1995; accepted 7 February 1996